Available online at www.sciencedirect.com
SCIENCE DIRECT®
Journal of Structural Biology 150 (2005) 170–179
Journal of Structural Biology
www.elsevier.com/locate/yjsbi

Filaments of the Ure2p prion protein have a cross-β core structure

Ulrich Baxa [a,b], Naiqian Cheng [a], Dennis C. Winkler [a], Thang K. Chiu [c], David R. Davies [c], Deepak Sharma [d], Hideyo Inouye [d], Daniel A. Kirschner [d], Reed B. Wickner [b], Alasdair C. Steven [a,*]

[a] *Laboratory of Structural Biology, National Institute of Arthritis, Musculoskeletal, and Skin Diseases, National Institutes of Health, Bethesda, MD 20892, USA*
[b] *Laboratory of Biochemistry and Genetics, National Institute of Diabetes and Digestive and Kidney Diseases, National Institutes of Health, Bethesda, MD 20892, USA*
[c] *Laboratory of Molecular Biology, National Institute of Diabetes and Digestive and Kidney Diseases, National Institutes of Health, Bethesda, MD 20892, USA*
[d] *Biology Department, Boston College, Chestnut Hill, MA 02467, USA*

Received 22 December 2004, and in revised form 5 February 2005
Available online 14 March 2005

Abstract

Formation of filaments by the Ure2 protein constitutes the molecular mechanism of the [URE3] prion in yeast. According to the "amyloid backbone" model, the N-terminal asparagine-rich domains of Ure2p polymerize to form an amyloid core fibril that is surrounded by C-terminal domains in their native conformation. Protease resistance and Congo Red binding as well as β-sheet content detected by spectroscopy—all markers for amyloid—have supported this model, as has the close resemblance between 40 Å N-domain fibrils and the fibrillar core of intact Ure2p filaments visualized by cryo-electron microscopy and scanning transmission electron microscopy. Here, we present electron diffraction and X-ray diffraction data from filaments of Ure2p, of N-domains alone, of fragments thereof, and of an N-domain-containing fusion protein that demonstrate in each case the 4.7 Å reflection that is typical for cross-β structure and highly indicative of amyloid. This reflection was observed for specimens prepared by air-drying with and without sucrose embedding. To confirm that the corresponding structure is not an artifact of air-drying, the reflection was also demonstrated for specimens preserved in vitreous ice. Local area electron diffraction and X-ray diffraction from partially aligned specimens showed that the 4.7 Å reflection is meridional and therefore the underlying structure is cross-β.
Published by Elsevier Inc.

Keywords: Electron diffraction; X-ray diffraction; Yeast prion; Natively unfolded protein

1. Introduction

The non-chromosomal element [URE3] in the yeast, *S. cerevisiae*, was identified as an aggregated, infectious (prion) form of the cytosolic protein Ure2p (Edskes et al., 1999; Masison and Wickner, 1995; Speransky et al., 2001; Wickner, 1994). The normal, soluble, form of Ure2p has a regulatory function in the nitrogen catabolite repression pathway (NCR)[1] (Cooper, 2002). When wild-type yeast cells are grown on a rich nitrogen source like ammonia, Ure2p binds to the transcription factor Gln3p and blocks its entry into the nucleus, thereby shutting off genes that are needed to utilize poor nitrogen sources (Beck and Hall, 1999; Blinder et al., 1996; Drillien et al., 1973). In [URE3] strains, this regulatory function is lost.

* Corresponding author. Fax: +1 301 443 7651.
E-mail address: Alasdair_Steven@nih.gov (A.C. Steven).

[1] *Abbreviations used:* GFP, green fluorescent protein; NCR, nitrogen catabolite repression.

1047-8477/$ - see front matter. Published by Elsevier Inc.
doi:10.1016/j.jsb.2005.02.007

The N-terminal domain of Ure2p (N-domain, residues 1–90) is both necessary and sufficient for prion conversion and propagation (Masison et al., 1997; Masison and Wickner, 1995), whereby Ure2p forms filaments in the infected cells (Speransky et al., 2001). Hence it is also referred to as the prion-forming domain or, simply, prion domain. This domain is unusually rich in the polar uncharged residues, asparagine, glutamine and serine. Yeast cells expressing only the C-terminal domain of Ure2p (residues 90–354) still have a functional, although somewhat leaky, NCR but are unable to convert to the [URE3] form (Maddelein and Wickner, 1999; Masison and Wickner, 1995). The crystal structure of the C-terminal domain has been solved (Bousset et al., 2001a; Umland et al., 2001), confirming the expectation based on sequence similarity that it has the same fold as glutathione *S*-transferase (Coschigano and Magasanik, 1991). In fact, the C-domain binds glutathione (Bousset et al., 2001b) and has glutathione peroxidase activity (Bai et al., 2004).

Recombinant Ure2p can also form filaments in vitro (Taylor et al., 1999), and in this form, retains both glutathione binding (Bousset et al., 2002) and glutathione peroxidase activity (Bai et al., 2004). These observations indicate that the C-terminal domains are still folded in the filamentous state of Ure2p, supporting the earlier inference to this effect based on the activities of various enzymes in filaments of fusion proteins in which they were coupled to the N-domain of Ure2p (Baxa et al., 2002). The inference that the C-domain remains folded in filaments is strongly supported by differential scanning calorimetry of Ure2p filaments, soluble Ure2p and soluble C-terminal domains (Baxa et al., 2004). The C-terminal domain responded to thermal perturbation in the same way in all three states, indicating that it does not change its structure upon entering filaments.

In the soluble state of Ure2p, the N-domain is natively unfolded, as attested by its sensitivity to proteases (Baxa et al., 2003; Thual et al., 1999), as well as data from physical chemistry (Galani et al., 2002; Perrett et al., 1999; Zhou et al., 2001), differential scanning calorimetry (Baxa et al., 2004), and NMR spectroscopy (Pierce et al., 2004). Upon entering the filamentous state, it undergoes a drastic conformational change as attested by its becoming highly resistant to proteases (Baxa et al., 2003; Ripaud et al., 2004; Taylor et al., 1999) and other lines of evidence (Baxa et al., 2004; Schlumpberger et al., 2000; Taylor et al., 1999). The predisposition for this conformational change seems to lie mainly in its amino acid composition, since five randomizations of the order of the amino acids of the N-domain sequence produced Ure2p variants that retained the ability to form filaments in vitro and become prions in vivo (Ross et al., 2004).

High resolution negative staining as well as cryo-electron microscopy showed that Ure2p filaments have a thin core fibril with globular domains arranged around it in a left handed spiral (Baxa et al., 2003; Kajava et al., 2004). In diameter and appearance, the core fibril matches fibrils assembled in vitro from N-domains, as well as residual filaments remaining after proteolysis of intact Ure2p filaments (Baxa et al., 2003; Taylor et al., 1999). The observations summarized above underlie the "amyloid backbone" model, whereby residues 1 to ~70 polymerize to form an amyloid filament that is surrounded by native C-terminal domains (residues ~90 to 354) and connected to them by a flexible linker (residues ~70 to ~90) (Baxa et al., 2002, 2003; Kajava et al., 2004; Speransky et al., 2001; Taylor et al., 1999).

The evidence that the core fibril is amyloid is extensive but somewhat circumstantial: (i) it is strikingly resistant to digestion with proteinase K (Baxa et al., 2003; Ripaud et al., 2004; Taylor et al., 1999); (ii) filaments of all N-domain-containing constructs examined to date bind Congo Red and show yellow-green birefringence (Baxa et al., 2003; Taylor et al., 1999); (iii) N-domain filaments are rich in β-structure and an increase of β-structure content has been observed upon filament formation by Ure2p (Schlumpberger et al., 2000; Taylor et al., 1999); and (iv) core fibrils are straight and smooth-sided (Taylor et al., 1999), and resemble in these respects other filaments accepted to be amyloids, e.g., Alzheimer β-peptide and amylin (Goldsbury et al., 1997, 2000). However, direct evidence from diffraction methods for the presence of cross-β structure has been lacking. Here we fill this gap by reporting electron diffraction and X-ray diffraction studies.

2. Experimental procedures

2.1. Preparation of Ure2p filaments

Protein was produced as described previously (Baxa et al., 2002, 2003; Speransky et al., 2001; Taylor et al., 1999). Filaments were made by incubation of protein solutions (usually at about 1 mg/ml) on a shaker for 16 h at 4 °C. Proteinase K-digested Ure2p filaments were produced as described (Baxa et al., 2003). Before filament preparations were used in experiments, they were sedimented repeatedly at 40 000*g* for 1 h at 4 °C to remove any soluble protein. Prior to air drying with or without sucrose embedding, filaments were taken up in water or very dilute buffer (<2 mM phosphate) to reduce diffraction from salt crystals after drying. At all times, the filaments were maintained at room temperature or 4 °C.

2.2. Electron microscopy and diffraction

Samples were negatively stained for assessment of yield and quality. Samples were adsorbed onto freshly glow-discharged carbon-coated grids, rinsed with water,

and stained with 1% uranyl acetate. For sucrose embedding, samples were mixed with an equal volume of 1% sucrose and adsorbed onto freshly glow-discharged carbon-coated grids. After 5 min, excess solution was blotted off and the sample was allowed to dry. Both kinds of specimens were examined in a CM120 microscope (FEI, Hillsboro, OR). For cryo-EM, drops of sample were adsorbed to holey carbon films, blotted, and vitrified by plunging into liquid ethane. These grids were examined in a CM200-FEG microscope (FEI, Hillsboro, OR) with a Gatan 626 cryo-holder (Cheng et al., 1999). Diffraction patterns were taken from areas of ~6 μm diameter for powder spectra and ~1 μm for micro-diffraction from locally ordered areas, with doses of 1–4 $e^-/Å^2$. Subsequently, one image was taken in defocused diffraction mode and another one in image mode of the area used for diffraction, to assess filament orientation and density. Diffraction spacings were calibrated with graphitized carbon, evaporated thallous chloride, and evaporated aluminium (Electron Microscopy Science, Hatfield, PA). Rotational registration between the diffraction pattern and the image was calibrated with a grid of negatively stained catalase crystals, prepared as described by Wrigley (1968).

2.3. X-ray diffraction and analysis

To prepare the Ure2p$^{10–39}$ specimen, lyophilized peptide was suspended in ultra-pure 18 MΩ water (U.S. Filter, Lowell, MA), vortexed, and briefly centrifuged at 16000*g* to sediment any precipitate. About 2–4 μL of the supernatant was then slowly drawn into a 0.5–0.7 mm-diameter siliconized, thin-walled glass capillary tube (Charles A. Supper, South Natick, MA), which was then sealed, and placed in a 2-Tesla permanent magnet (Charles A. Supper; Oldenbourgh and Phillips, 1986). A pin-hole was punched through the wax at the wide end of the capillary to allow gradual drying (under ambient temperature and humidity) of the solution over 1–2 weeks. When the sample was a small uniform disk, the capillary tube was removed from the magnetic field and transferred to the sample holder for analysis by X-ray diffraction. The Ure2p$^{1–89}$ filament sample was examined as a wet concentrated pellet after sealing in a capillary tube.

Diffraction patterns were recorded on Kodak DEF film using double mirror focused CuKα radiation generated by an Elliot GX-20 rotating anode (Marconi Avionics, UK). The specimen-to-film distances of the X-ray cameras were calibrated using known standards (calcite, $d = 3.035$ Å; NaCl, $d = 2.821$ Å). Exposure time ranged from one to three days and the observed spacings were calculated using Bragg's law from positions of the reflections measured directly off the film. The diffraction patterns were digitized using ScanMaker 5 (Microtek Laboratory, 3715 Doolittle Drive, Redondo Beach, CA, USA). The ScanMaker 5, using 300 dpi (corresponding to 84.66 μm pixels), was operated using MacIntosh program ScanWizard PPC 3.2.2. The machine readout was calibrated using the known optical density of a Kodak Step Calibration Tablet (No.2; range from 0.04 to 3.03 OD). The digitized image was displayed on NIH IMAGE (developed at the U.S. National Institutes of Health, and available at http://rsb.info.nih.gov/nih-image/). The intensities along the equatorial direction and radial direction crossing the off-meridional intensity maximum were plotted by selecting narrow windows. The background curves were approximated as polynomials and subtracted from the measured intensity. Each reflection was assumed to be a Gaussian function. Measurements of the integral widths and integral intensities of the reflections were obtained by fitting the background corrected intensity profile to multiple Gaussian functions. The integral width of the direct beam, determined after Gaussian approximation, was 397 μm for the Ure2p$^{10–39}$ sample, and 332 μm for Ure2p$^{1–89}$ which correspond to 2.95×10^{-3} $Å^{-1}$ and 2.46×10^{-3} $Å^{-1}$.

Samples of Ure2p full-length filaments were dried in bromosilicate capillaries (Charles Supper, Natick, MA) with or without a magnetic field (~1.5 T). X-ray diffraction images were recorded using a Rigaku rotating anode source (CuKα) and a Raxis IV++ detector. Exposure times were 5–15 min at a specimen to detector distance of 71.2 mm.

3. Results

Recombinant Ure2p forms filaments under physiological buffer conditions (Taylor et al., 1999). Rigorous proteinase K treatment digests away the C-domains, leaving thin fibrils composed of N-terminal material (Baxa et al., 2003). The N-domain alone fibrillizes rapidly in physiological buffers (Taylor et al., 1999), as do N-domain fragments, e.g., Ure2p$^{10–39}$ (Kajava et al., 2004). Moreover, fusion proteins in which the C-domain is exchanged for other globular proteins such as the green fluorescent protein (GFP) readily form filaments (Baxa et al., 2002). We set out to investigate filaments of all these kinds by diffraction analysis.

3.1. Electron diffraction

Electron diffraction has been used on previous occasions to detect repetitive secondary structures in protein filaments (e.g. Watts et al., 1998), including cross-β structure in amyloids (King and Diaz-Avalos, 2004; Serpell et al., 2000). It has the advantage that it is highly sensitive; moreover, since filaments tend to be deposited on EM grids so as to present side-views, Bragg-angle sampling of axial periodicities occurs for a larger fraction of the sample than for a three-dimensional pellet of randomly oriented filaments.

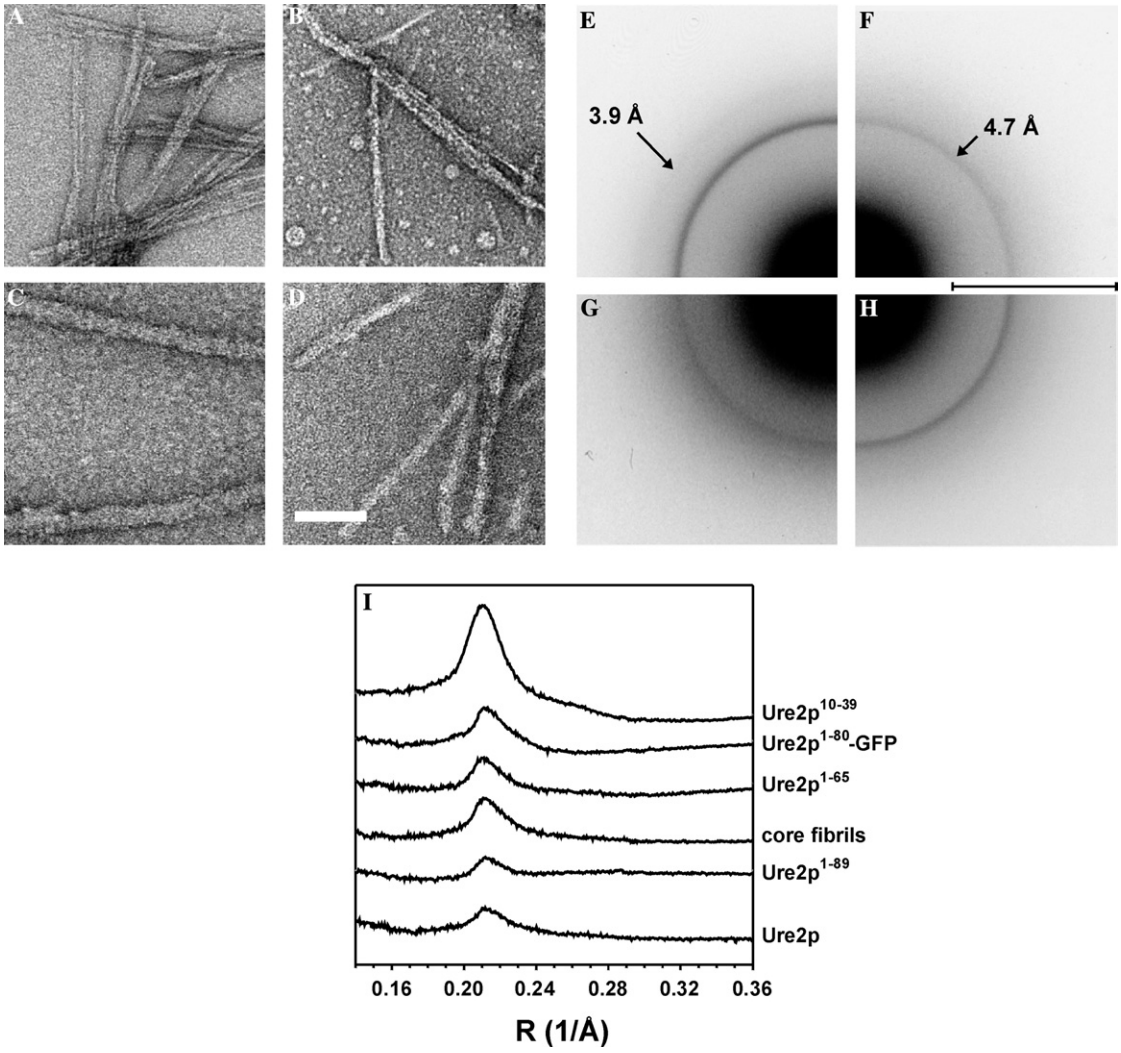

Fig. 1. Electron diffraction analysis of six kinds of Ure2p-related filaments. The preparations of filaments were first checked by negative stain electron microscopy. Four examples are shown: (A) Ure2p$^{10–39}$; (B) Ure2p$^{1–65}$; (C) full-length Ure2p; and (D) Ure2p$^{1–89}$. EM grids bearing sucrose-embedded specimens were then examined by electron diffraction. Quarter-plane patterns corresponding to samples (A–D) are shown in (E–H), respectively. The spectra were digitized and azimuthally averaged. Similar analyses were also performed for filaments of the Ure2p$^{1–80}$-GFP fusion protein, and for core fibrils remaining after proteinase K digestion of Ure2p filaments. The resulting traces between spatial frequencies indicated below (F) from 1/(7.1 Å) to 1/(2.77 Å) are shown in (I). From the top, they are from: Ure2p$^{10–39}$, Ure2p$^{1–80}$-GFP, Ure2p$^{1–65}$, core fibrils; Ure2p$^{1–89}$, and Ure2p. In each case, a prominent reflection at ~0.21 Å^{-1} or 1/(4.7 Å) was detected.

Filaments of Ure2p, Ure2p$^{1–65}$, Ure2p$^{1–89}$, Ure2p$^{10–39}$ and Ure2p$^{1–80}$-GFP, as well as Ure2p core fibrils produced by proteinase K digestion, were embedded in sucrose on carbon film-bearing EM grids (see Section 2) and examined in the electron microscope. In each case, the grids were scanned for promising areas and electron diffractograms were recorded from areas of ~6 μm to ~1 μm across, and images of these areas were then recorded after suitably defocusing the diffracted electron beam (Fig. 1). Strong diffraction rings at a spacing of 4.7 Å were observed in all cases, but were not seen in control grids prepared with soluble Ure2p or with sucrose solution alone (data not shown). Ure2p$^{10–39}$ filaments produced the strongest reflections and for these specimens, an additional ring at 3.85 Å (Fig. 1E) was observed. In one case, the second order of the 4.7 Å reflection was also observed (data not shown). As expected for a protein-associated feature, the 4.7 Å reflection was radiation-sensitive and decayed completely after a dose of ~25 e^{-}/Å^2, even though the overall appearance of the filaments in the accompanying images was unaltered.

We used sucrose embedding to prepare these samples since this treatment has been observed to mitigate drying-induced damage to native protein structure (Akey and Edelstein, 1983; Bourguignon et al., 1978; Kessel et al., 1986; Tokuyasu, 1973). However, we obtained essentially the same results when samples were air-dried without embedding in sucrose (data not shown), indicating that the structure responsible for generating the 4.7 Å

diffraction ring is quite robust and survives drying. This finding was not surprising, since N-domain filaments are highly resistant to proteinase K treatment and to heating to 105 °C in buffer (Baxa et al., 2004), and even resist boiling in 2% SDS (Baxa et al., 2003; Ripaud et al., 2004; Speransky et al., 2001). Notwithstanding, all filament preparations for diffraction were kept between 4 °C and room temperature at all times except when vitrified (see below).

To address the possibility that—despite the evidence summarized above (see Section 1)—filaments of intact Ure2p may somehow lack amyloid (e.g., their core fibrils have some other structure) and the β-structures that generate their 4.7 Å reflection arise from denaturation of their N-domains and/or their C-domains (Bousset et al., 2003, see Section 4), we prepared vitrified specimens of these filaments and, for reference, also of Ure2p$^{10–39}$ filaments. The method of preparing samples in thin films of vitreous ice is known to preserve the native structure of proteins (Al-Amoudi et al., 2004; Dubochet et al., 1981, 1988; Lepault et al., 1983). Diffraction from vitreous ice itself produces a weak, broad reflection at 3.7 Å and an even weaker one at 2.2 Å (Al-Amoudi et al., 2002; Dowell and Rinfret, 1960; McDowall et al., 1983). In addition to these reflections, we observed diffraction rings at 3.67, 2.25, and 1.92 Å from cubic ice crystals that condensed on the specimen during cryo-transfer into the electron microscope.

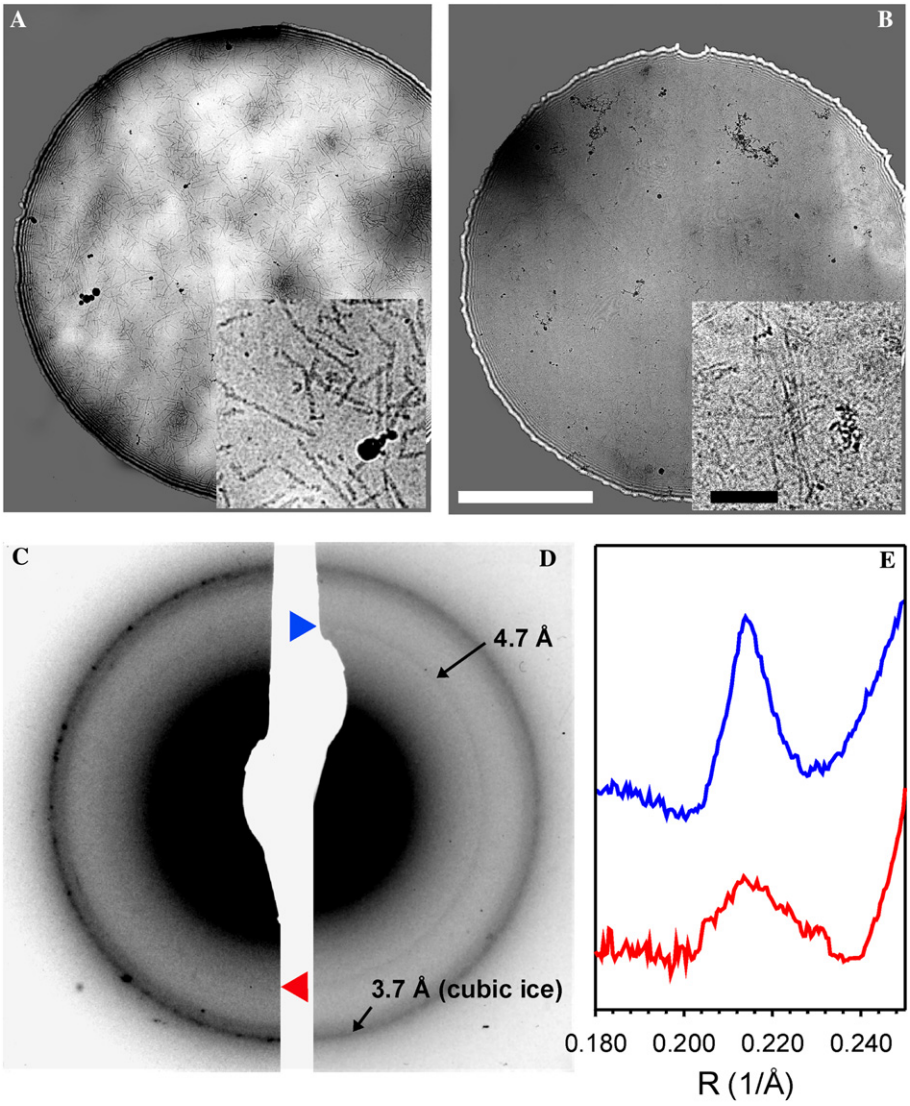

Fig. 2. Electron diffraction analysis of Ure2p-related filaments embedded in vitreous ice. (A and B) Images of the areas from which the diffraction patterns (C) and (D), respectively, were recorded. The specimens were (A) Ure2p filaments, and (B) Ure2p$^{10–39}$ filaments. At bottom right in (A) and (B) are shown blow-ups of small areas. The micrographs are heavily defocussed. The calibration bars represent 1.5 μm for the full size areas and 250 nm for the blowups. The most prominent features of the diffraction patterns are rings at 3.7 Å which correspond to the strong (1 1 1) reflection of contaminating cubic ice crystals that are visible as small dark flecks in (A) and (B). However, both samples also exhibit a diffraction ring at 4.7 Å that is further illustrated on (E) in azimuthally averaged, baseline corrected scans: Ure2p filaments—red; Ure2p$^{10–39}$ filaments—blue.

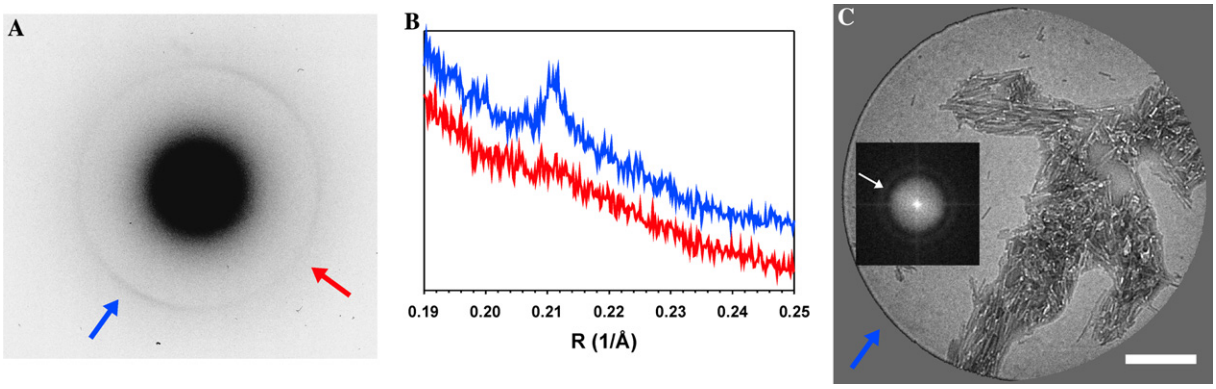

Fig. 3. Selected area electron diffraction of Ure2p$^{10–39}$ filaments. (A) The diffraction pattern recorded from the field imaged in (C) in which there is a preferential alignment of the filaments. The strength of the 4.7 Å ring in the diffraction pattern (A) is anisotropic. The colored arrows indicate the direction of line scans shown in (B): blue—direction of maximum intensity; red—direction of minimum intensity. (C) Image of the field diffracted in (A). The majority of filaments are approximately oriented in the direction indicated by the blue arrow. The inset shows a calculated diffraction pattern of the filament-containing area in the digitized image. Inside the first zero of the contrast transfer function (inner dark ring), the intensity of the calculated diffraction pattern is anisotropic in a manner that anti-correlates with that of the electron diffraction pattern, i.e., the maximum intensity aligns with the direction of minimum intensity in the 4.7 Å ring. This is the expected intensity distribution in a Fourier transform of a field of partially aligned rods.

Despite this background, we were able to identify a sharp ring at 4.7 Å for both specimens (Fig. 2). Although unmistakably present, this signal is weaker in the Ure2p diffractogram, which we attribute to several factors: (i) counting filaments in both optical fields gave ~4-fold fewer filaments for Ure2p than Ure2p$^{10–39}$. In contrast to Ure2p filaments, the Ure2p$^{10–39}$ filaments are thin and have a marked tendency to bundle, so that this count is a low estimate of the real number; (ii) the inferred amyloid component accounts for only about 20% of the mass of a Ure2p filament. In general, we found producing thin ice films from drops of concentrated Ure2p filament preparations to be problematic on account of their tendency to precipitate into large clumps. Through surface tension effects, these clumps tended to prevent obtaining ice layers that were thin enough to be well suited for electron microscopy and diffraction experiments. Moreover, in clumps the majority of filaments would not be oriented perpendicular to the electron beam (see above).

The same effect—filament stickiness—probably explains why we did not succeed in aligning filaments on a larger scale to confirm the expectation that the 4.7 Å peak represents a meridional reflection. Accordingly, we reverted to another approach—of scanning grids of sucrose-embedded Ure2p$^{10–39}$ filaments (which gave the strongest signal)—for small areas where there happened to be a predominant local orientation of the filaments. Fig. 3 shows the result of such an experiment. The 4.7 Å reflection is markedly stronger in the direction in which most of the filaments are pointing. Their preferred orientation was confirmed by the computed power spectrum of the image, which showed a stronger signal in the direction perpendicular to the filament orientation (cf. Fig. 3C, inset). Thus, we conclude that the 4.7 Å reflection is meridional.

3.2. X-ray diffraction

Filaments of Ure2p$^{10–39}$, Ure2p$^{1–89}$, and Ure2p were dried in capillaries at room temperature and subjected to X-ray diffraction analysis. The samples showed a strong sharp peak at 4.7 Å as well as weaker and broader peaks at ~10 and ~3.85 Å—Fig. 4. (The latter two reflections were marginal in the experiment with Ure2p$^{1–89}$). In a control experiment in which the sample was made from a C-domain preparation, i.e., Ure2p$^{65–354}$, no diffraction rings were detected (data not shown).

The richest pattern was one obtained with Ure2p$^{10–39}$ filaments (Figs. 4A, B and D, top and inset). In addition to the dominant ring at 4.7 Å, it exhibits a clear outer ring at 3.85 Å. A meridional reflection at this spacing has been detected in diffractograms of other aligned amyloid fibrils (Inouye et al., 1993; Inouye and Kirschner, 1997; Sumner Makin and Serpell, 2004) and is also indicative of cross-β structure. This sample also showed a broad but well defined ring at 10 Å. Again, reflections at this spacing have been detected in diffraction from other amyloids, and with aligned specimens, they have been found to be equatorial reflections and interpreted as the inter-sheet spacing in parallel packings. The pattern has two additional rings at spacings of 17.1 and 30.7 Å (Figs. 4B and D, inset), whose interpretation is considered further below (Section 4).

In one experiment, intact Ure2p filaments were dried in a magnetic field, producing a predominant orientation in the sample that was reflected in anisotropic diffraction rings (Fig. 4E). These data showed that the repeats that gave rise to the 4.7 Å ring are oriented perpendicular to those that generate the 10 Å reflection. Since the 4.7 Å reflection is meridional (see above, Fig. 3), the 10 Å reflection should be equatorial.

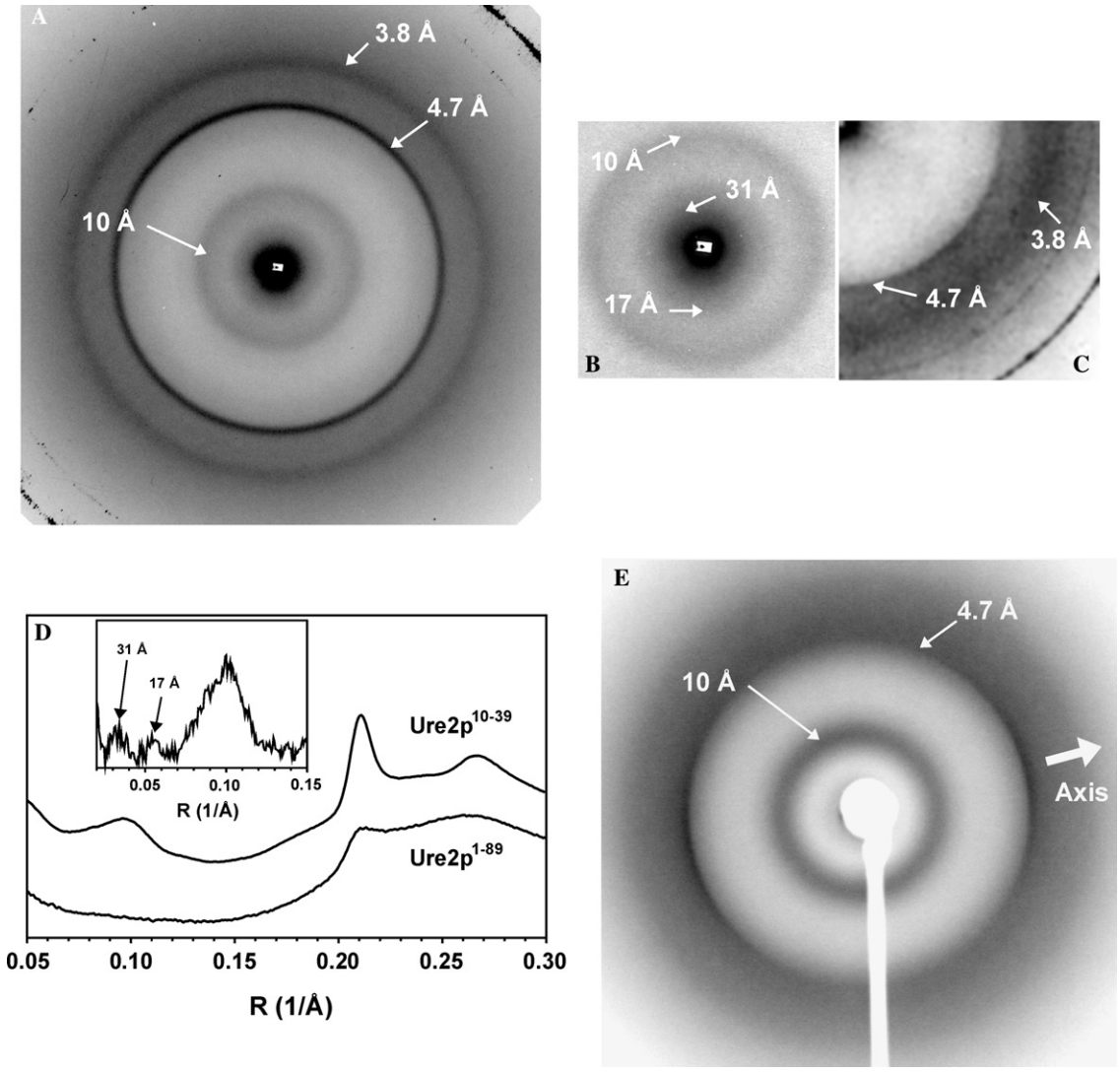

Fig. 4. X-ray diffraction patterns from several kinds of Ure2p-related filaments. (A) Diffraction from Ure2p$^{10–39}$ sample dried in a magnetic field (96 h exposure). (B) Enlargement of the low-angle region, including the rings at 17 Å and (overexposed) 31 Å; (C) diffraction from pellet containing Ure2p$^{1–89}$ filaments (91 h exposure). The 4.7 Å and 3.85 Å rings are marked with arrows. (D) Azimuthally averaged intensity traces between spacings of 1/(20 Å) and 1/(3.3 Å) for the diffraction patterns from Ure2p$^{10–39}$ (top), Ure2p$^{1–89}$ (bottom). The inset shows a baseline corrected trace from Ure2p$^{10–39}$ in the low angle range from 1/(50 Å) to 1/(6.7 Å) where the 32 Å and the 17 Å reflection are visible as small peaks. (E) Diffraction from a sample of partially oriented Ure2p filaments. The direction of strongest intensity for the 4.7 Å ring is perpendicular to the direction of strongest intensity for the 10 Å ring, consistent with them representing meridional and equatorial reflections, respectively.

4. Discussion

In this study, we used electron diffraction and X-ray diffraction to investigate Ure2p-related filaments under several conditions—after air-drying, sucrose embedding, and vitrification. X-ray fiber diffraction has a long history of applications to detect cross-β structure in amyloid filaments (Bonar et al., 1969; Kirschner et al., 1986; Sipe and Cohen, 2000). However, electron diffraction has complementary advantages of sensitivity and applicability to specimens that exhibit poor long-range order. This technique has recently been used to demonstrate cross-β structure in filaments of α-synuclein, tau, amylin (IAPP), and Sup35p (Berriman et al., 2003; King and Diaz-Avalos, 2004; Serpell et al., 2000; Sumner Makin and Serpell, 2004).

The typical diffraction signature for amyloids is a meridional reflection at 4.7 Å, representing the spacing between β-strands running perpendicular to the filament axis. A generally weaker and broader equatorial reflection may be observed at ~10 Å that represents the inter-sheet spacing, and another meridional reflection at 3.85 Å that also relates to β-sheet structure (Kirschner et al., 1987; Makin and Serpell, 2002). We observed the 4.7 Å reflection in all samples analyzed. The 3.85 Å reflection was detected by both techniques for our best aligned specimens. The 10 Å reflection was presumably submerged in the forward scattering peak of the electron diffractograms but was observed in X-ray diffraction of both Ure2p$^{10–39}$ and Ure2p filaments (Fig. 4).

Taken together, these experiments demonstrated cross-β structure in all N-domain-containing filaments analyzed. This trend substantiates the thesis that the Ure2p N-domains have essentially the same amyloid fold whether they are in N-domain filaments, core fibrils remaining after digesting Ure2p filaments, or filaments of intact Ure2p or of the N-domain-GFP fusion protein.

In a recent paper, Bousset et al. reported X-ray fiber diffraction experiments from air-dried Ure2p filaments in which they did not observe a reflection at 4.7 Å unless they heated the sample at 60 °C (Bousset et al., 2003). Instead they presented a photograph of a broad intensity peak extending from about 5.0 to about 3.3 Å (Fig. 3B in Bousset et al., 2003). No radial densitometric traces were reported. However, failure to observe a reflection in an experiment of this kind does not necessarily imply that the corresponding structure is absent (Agianian et al., 1999): it may simply result from an insufficient number of filaments being oriented perpendicular to the beam in the portion of specimen sampled. The main features of the pattern that was observed after incubating the filaments at 60 °C for 1 h were also present in the one that we observed without any such heating (Fig. 4). Since 60 °C is below the threshold for thermal denaturation of the C-terminal domain and N-domain filaments show no thermal events up to 105 °C (Baxa et al., 2004), we suspect that these authors may simply have observed an amplification of a pre-existing signal through a fortuitous improvement of the alignment in this specimen as it was heated or dried.

In particular, having observed the 4.7 Å reflection in electron diffraction from Ure2p filaments preserved in vitreous ice, we conclude that this feature is not caused by denaturation. Furthermore, we attribute the 4.7 Å reflection to the N-domain amyloid core of intact Ure2p filaments on the basis of the following arguments: (i) there is essentially no β-structure in natively folded C-domains (Bousset et al., 2001a; Umland et al., 2001) and (ii) we observed the same reflection in several other kinds of N-domain-containing filaments.

4.1. The parallel super-pleated β-structure model

Recently, a structure has been proposed for the amyloid core of Ure2p filaments in which individual N-domains assuming a planar serpentine fold are stacked axially (Kajava et al., 2004). This arrangement, which generates an array of parallel β-sheets in cross-β-conformation, is consistent with the observed reflections at 4.7, 3.85, and 10 Å. An energy-minimized model was calculated for the Ure2p$^{10–39}$ segment, which is described as four β-strands of equal length, so that in cross-section, it has dimensions of ~35 by 30 Å. These dimensions are consistent with the two lower-angle reflections observed in X-ray diffraction of this sample, i.e., they may be indexed as the (10) and (11) reflections for a two-dimensional hexagonal lattice (which may be either paracrystalline or simply hexagonal close packing) with an average lattice constant of ~35 Å, such that the (10) is at ~35 × 3/2 Å (= 30.3 Å cf. 30.7 Å), and (11) is at ~35/2 Å (= 17.5 Å cf. 17.1 Å). An alternative interpretation is that the two reflections may correspond to the two intensity maxima at $R = 0.82/r$ and $1.34/r$ in the Fourier transform of a solid cylinder of radius r. However, the observed spacings would specify a diameter of ~50 Å, which is considerably larger than the 35 Å that would be required to accommodate the given mass at typical protein density, if there is one copy of Ure2p$^{10–39}$ per 4.7 Å axial step as in other N-domain-related filaments (Baxa et al., 2003). Accordingly, we incline to the former interpretation.

4.2. Backbone structures

Filaments from another yeast prion protein, Sup35p, have already been shown to have cross-β structure by X-ray diffraction (King and Diaz-Avalos, 2004; Kishimoto et al., 2004; Serio et al., 2000). These and other observations point to the likelihood of a generally similar mechanism of prion conversion in this system, whereby the N-terminal domain or domains of Sup35p polymerize to form an amyloid backbone which is surrounded by the functional C-terminal domains. The latter domains normally play a role in termination of transcription, although it remains to be established whether they retain their native conformation when they enter the filamentous state and consequently whether their inactivation is the result of a steric mechanism as it is with Ure2p. Indeed, arrangements whereby the N- and M-domains of Sup35p form the filament backbone have been envisaged for some time (Glover et al., 1997; King and Diaz-Avalos, 2004; Tanaka et al., 2004). Recently, more detailed models have been proposed, one based on bundles of stacked β-helical polymers (Kishimoto et al., 2004), and another a variant of the superpleated β-sheet structure (Kajava et al., 2004). Both can account for the observed cross-β pattern observed by X-ray fiber diffraction (Kishimoto et al., 2004) and discrimination between them must rely on other experimentally determined constraints.

Acknowledgments

We thank Andrey Kajava, Louise Serpell, Thusnelda Stromer, and Sumner Makin for helpful discussions and Wai-Ming Yau and Robert Tycko for synthesizing the Ure2p$^{10–39}$ peptide. Research at Boston College was supported by an Alzheimer's Association/T.L.L. Temple Discovery Award (to D.A.K.), and by institutional support from Boston College.

References

Agianian, B., Leonard, K., Bonte, E., Van der Zandt, H., Becker, P.B., Tucker, P.A., 1999. The glutamine-rich domain of the *Drosophila* GAGA factor is necessary for amyloid fibre formation in vitro, but not for chromatin remodelling. J. Mol. Biol. 285, 527–544.

Akey, C.W., Edelstein, S.J., 1983. Equivalence of the projected structure of thin catalase crystals preserved for electron microscopy by negative stain, glucose or embedding in the presence of tannic acid. J. Mol. Biol. 163, 575–612.

Al-Amoudi, A., Dubochet, J., Studer, D., 2002. Amorphous solid water produced by cryosectioning of crystalline ice at 113 K. J. Microsc. 207, 146–153.

Al-Amoudi, A., Norlen, L.P., Dubochet, J., 2004. Cryo-electron microscopy of vitreous sections of native biological cells and tissues. J. Struct. Biol. 148, 131–135.

Bai, M., Zhou, J.M., Perrett, S., 2004. The yeast prion protein Ure2 shows glutathione peroxidase activity in both native and fibrillar forms. J. Biol. Chem. 279, 50025–50030.

Baxa, U., Ross, P.D., Wickner, R.B., Steven, A.C., 2004. The N-terminal prion domain of Ure2p converts from an unfolded to a thermally resistant conformation upon filament formation. J. Mol. Biol. 339, 259–264.

Baxa, U., Speransky, V., Steven, A.C., Wickner, R.B., 2002. Mechanism of inactivation on prion conversion of the *Saccharomyces cerevisiae* Ure2 protein. Proc. Natl. Acad. Sci. USA 99, 5253–5260.

Baxa, U., Taylor, K.L., Wall, J.S., Simon, M.N., Cheng, N., Wickner, R.B., Steven, A.C., 2003. Architecture of Ure2p prion filaments: the N-terminal domains form a central core fiber. J. Biol. Chem. 278, 43717–43727.

Beck, T., Hall, M.N., 1999. The TOR signalling pathway controls nuclear localization of nutrient-regulated transcription factors. Nature 402, 689–692.

Berriman, J., Serpell, L.C., Oberg, K.A., Fink, A.L., Goedert, M., Crowther, R.A., 2003. Tau filaments from human brain and from in vitro assembly of recombinant protein show cross-beta structure. Proc. Natl. Acad. Sci. USA 100, 9034–9038.

Blinder, D., Coschigano, P.W., Magasanik, B., 1996. Interaction of the GATA factor Gln3p with the nitrogen regulator Ure2p in *Saccharomyces cerevisiae*. J. Bacteriol. 178, 4734–4736.

Bonar, L., Cohen, A.S., Skinner, M.M., 1969. Characterization of the amyloid fibril as a cross-beta protein. Proc. Soc. Exp. Biol. Med. 131, 1373–1375.

Bourguignon, L.Y., Tokuyasu, K.T., Singer, S.J., 1978. The capping of lymphocytes and other cells, studied by an improved method for immunofluorescence staining of frozen sections. J. Cell. Physiol. 95, 239–257.

Bousset, L., Belrhali, H., Janin, J., Melki, R., Morera, S., 2001a. Structure of the globular region of the prion protein Ure2 from the yeast *Saccharomyces cerevisiae*. Structure 9, 39–46.

Bousset, L., Belrhali, H., Melki, R., Morera, S., 2001b. Crystal structures of the yeast prion Ure2p functional region in complex with glutathione and related compounds. Biochemistry 40, 13564–13573.

Bousset, L., Briki, F., Doucet, J., Melki, R., 2003. The native-like conformation of Ure2p in fibrils assembled under physiologically relevant conditions switches to an amyloid-like conformation upon heat-treatment of the fibrils. J. Struct. Biol. 141, 132–142.

Bousset, L., Thomson, N.H., Radford, S.E., Melki, R., 2002. The yeast prion Ure2p retains its native alpha-helical conformation upon assembly into protein fibrils in vitro. EMBO J. 21, 2903–2911.

Cheng, N., Conway, J.F., Watts, N.R., Hainfeld, J.F., Joshi, V., Powell, R.D., Stahl, S.J., Wingfield, P.E., Steven, A.C., 1999. Tetrairidium, a four-atom cluster, is readily visible as a density label in three-dimensional cryo-EM maps of proteins at 10–25 Å resolution. J. Struct. Biol. 127, 169–176.

Cooper, T.G., 2002. Transmitting the signal of excess nitrogen in *Saccharomyces cerevisiae* from the Tor proteins to the GATA factors: connecting the dots. FEMS Microbiol. Rev. 26, 223–238.

Coschigano, P.W., Magasanik, B., 1991. The URE2 gene product of *Saccharomyces cerevisiae* plays an important role in the cellular response to the nitrogen source and has homology to glutathione S-transferases. Mol. Cell. Biol. 11, 822–832.

Dowell, L.G., Rinfret, A.P., 1960. Low-temperature forms of ice as studied by X-ray diffraction. Nature 188, 1144–1148.

Drillien, R., Aigle, M., Lacroute, F., 1973. Yeast mutants pleiotropically impaired in the regulation of the two glutamate dehydrogenases. Biochem. Biophys. Res. Commun. 53, 367–372.

Dubochet, J., Adrian, M., Chang, J.J., Homo, J.C., Lepault, J., McDowall, A.W., Schultz, P., 1988. Cryo-electron microscopy of vitrified specimens. Q. Rev. Biophys. 21, 129–228.

Dubochet, J., Booy, F.P., Freeman, R., Jones, A.V., Walter, C.A., 1981. Low temperature electron microscopy. Annu. Rev. Biophys. Bioeng. 10, 133–149.

Edskes, H.K., Gray, V.T., Wickner, R.B., 1999. The [URE3] prion is an aggregated form of Ure2p that can be cured by overexpression of Ure2p fragments. Proc. Natl. Acad. Sci. USA 96, 1498–1503.

Galani, D., Fersht, A.R., Perrett, S., 2002. Folding of the yeast prion protein Ure2: kinetic evidence for folding and unfolding intermediates. J. Mol. Biol. 315, 213–227.

Glover, J.R., Kowal, A.S., Schirmer, E.C., Patino, M.M., Liu, J.J., Lindquist, S., 1997. Self-seeded fibers formed by Sup35, the protein determinant of [PSI+], a heritable prion-like factor of *S. cerevisiae*. Cell 89, 811–819.

Goldsbury, C.S., Cooper, G.J., Goldie, K.N., Muller, S.A., Saafi, E.L., Gruijters, W.T., Misur, M.P., Engel, A., Aebi, U., Kistler, J., 1997. Polymorphic fibrillar assembly of human amylin. J. Struct. Biol. 119, 17–27.

Goldsbury, C.S., Wirtz, S., Muller, S.A., Sunderji, S., Wicki, P., Aebi, U., Frey, P., 2000. Studies on the in vitro assembly of Aβ 1-40: implications for the search for a beta fibril formation inhibitors. J. Struct. Biol. 130, 217–231.

Inouye, H., Fraser, P.E., Kirschner, D.A., 1993. Structure of beta-crystallite assemblies formed by Alzheimer beta-amyloid protein analogues: analysis by X-ray diffraction. Biophys. J. 64, 502–519.

Inouye, H., Kirschner, D.A., 1997. X-ray diffraction analysis of scrapie prion: intermediate and folded structures in a peptide containing two putative alpha-helices. J. Mol. Biol. 268, 375–389.

Kajava, A.V., Baxa, U., Wickner, R.B., Steven, A.C., 2004. A model for Ure2p prion filaments and other amyloids: the parallel superpleated β-structure. Proc. Natl. Acad. Sci. USA 101, 7885–7890.

Kessel, M., Buhle, E.L., Glavaris, E., Aebi, U., 1986. A novel method for preventing collapse of air-dried specimens for heavy metal shadowing. In: Proceedings of the 44th Annual Meeting of EMSA. San Francisco Press, San Francisco, pp. 228–229.

King, C.Y., Diaz-Avalos, R., 2004. Protein-only transmission of three yeast prion strains. Nature 428, 319–323.

Kirschner, D.A., Abraham, C., Selkoe, D.J., 1986. X-ray diffraction from intraneuronal paired helical filaments and extraneuronal amyloid fibers in Alzheimer disease indicates cross-beta conformation. Proc. Natl. Acad. Sci. USA 83, 503–507.

Kirschner, D.A., Inouye, H., Duffy, L.K., Sinclair, A., Lind, M., Selkoe, D.J., 1987. Synthetic peptide homologous to beta protein from Alzheimer disease forms amyloid-like fibrils in vitro. Proc. Natl. Acad. Sci. USA 84, 6953–6957.

Kishimoto, A., Hasegawa, K., Suzuki, H., Taguchi, H., Namba, K., Yoshida, M., 2004. Beta-Helix is a likely core structure of yeast prion Sup35 amyloid fibers. Biochem. Biophys. Res. Commun. 315, 739–745.

Lepault, J., Booy, F.P., Dubochet, J., 1983. Electron microscopy of frozen biological suspensions. J. Microsc. 129, 89–102.

Maddelein, M.L., Wickner, R.B., 1999. Two prion-inducing regions of Ure2p are nonoverlapping. Mol. Cell. Biol. 19, 4516–4524.

Makin, O.S., Serpell, L.C., 2002. Examining the structure of the mature amyloid fibril. Biochem. Soc. Trans. 30, 521–525.

Masison, D.C., Maddelein, M.L., Wickner, R.B., 1997. The prion model for [URE3] of yeast: spontaneous generation and requirements for propagation. Proc. Natl. Acad. Sci. USA 94, 12503–12508.

Masison, D.C., Wickner, R.B., 1995. Prion-inducing domain of yeast Ure2p and protease resistance of Ure2p in prion-containing cells. Science 270, 93–95.

McDowall, A.W., Chang, J.J., Freeman, R., Lepault, J., Walter, C.A., Dubochet, J., 1983. Electron microscopy of frozen hydrated sections of vitreous ice and vitrified biological samples. J. Microsc. 131, 1–9.

Oldenbourgh, R., Phillips, W.C., 1986. Small permanent magnet for fields up to 2.6 T. Rev. Sci. Instrum. 57, 2362–2365.

Perrett, S., Freeman, S.J., Butler, P.J., Fersht, A.R., 1999. Equilibrium folding properties of the yeast prion protein determinant Ure2. J. Mol. Biol. 290, 331–345.

Pierce, M.M., Baxa, U., Steven, A.C., Bax, A., Wickner, R.B., 2004. Is the prion domain of soluble Ure2p unstructured? Biochemistry 44, 321–328.

Ripaud, L., Maillet, L., Immel-Torterotot, F., Durand, F., Cullin, C., 2004. The [URE3] yeast prion results from protein aggregates that differ from amyloid filaments formed in vitro. J. Biol. Chem. 279, 50962–50968.

Ross, E.D., Baxa, U., Wickner, R.B., 2004. Scrambled prion domains form prions and amyloid. Mol. Cell. Biol. 24, 7206–7213.

Schlumpberger, M., Wille, H., Baldwin, M.A., Butler, D.A., Herskowitz, I., Prusiner, S.B., 2000. The prion domain of yeast Ure2p induces autocatalytic formation of amyloid fibers by a recombinant fusion protein. Protein Sci. 9, 440–451.

Serio, T.R., Cashikar, A.G., Kowal, A.S., Sawicki, G.J., Moslehi, J.J., Serpell, L., Arnsdorf, M.F., Lindquist, S.L., 2000. Nucleated conformational conversion and the replication of conformational information by a prion determinant. Science 289, 1317–1321.

Serpell, L.C., Berriman, J., Jakes, R., Goedert, M., Crowther, R.A., 2000. Fiber diffraction of synthetic alpha-synuclein filaments shows amyloid-like cross-beta conformation. Proc. Natl. Acad. Sci. USA 97, 4897–4902.

Sipe, J.D., Cohen, A.S., 2000. Review: history of the amyloid fibril. J. Struct. Biol. 130, 88–98.

Speransky, V.V., Taylor, K.L., Edskes, H.K., Wickner, R.B., Steven, A.C., 2001. Prion filament networks in [URE3] cells of *Saccharomyces cerevisiae*. J. Cell Biol. 153, 1327–1336.

Sumner Makin, O., Serpell, L.C., 2004. Structural characterisation of islet amyloid polypeptide fibrils. J. Mol. Biol. 335, 1279–1288.

Tanaka, M., Chien, P., Naber, N., Cooke, R., Weissman, J.S., 2004. Conformational variations in an infectious protein determine prion strain differences. Nature 428, 323–328.

Taylor, K.L., Cheng, N., Williams, R.W., Steven, A.C., Wickner, R.B., 1999. Prion domain initiation of amyloid formation in vitro from native Ure2p. Science 283, 1339–1343.

Thual, C., Komar, A.A., Bousset, L., Fernandez-Bellot, E., Cullin, C., Melki, R., 1999. Structural characterization of *Saccharomyces cerevisiae* prion-like protein Ure2. J. Biol. Chem. 274, 13666–13674.

Tokuyasu, K.T., 1973. A technique for ultracryotomy of cell suspensions and tissues. J. Cell Biol. 57, 551–565.

Umland, T.C., Taylor, K.L., Rhee, S., Wickner, R.B., Davies, D.R., 2001. The crystal structure of the nitrogen regulation fragment of the yeast prion protein Ure2p. Proc. Natl. Acad. Sci. USA 98, 1459–1464.

Watts, N.R., Misra, M., Wingfield, P.T., Stahl, S.J., Cheng, N., Trus, B.L., Steven, A.C., Williams, R.W., 1998. Three-dimensional structure of HIV-1 Rev protein filaments. J. Struct. Biol. 121, 41–52.

Wickner, R.B., 1994. [URE3] as an altered URE2 protein: evidence for a prion analog in *Saccharomyces cerevisiae*. Science 264, 566–569.

Wrigley, N., 1968. The lattice spacing of crystalline catalase as an internal standard of length in electron microscopy. J. Ultrastruct. Res. 24, 454–464.

Zhou, J.M., Zhu, L., Balny, C., Perrett, S., 2001. Pressure denaturation of the yeast prion protein Ure2. Biochem. Biophys. Res. Commun. 287, 147–152.